Heavy Quark and Target Mass Effects on the Virtual Photon in QCD

Yoshio Kitadono[1], *Takahiro Ueda*[2], *Tsuneo Uematsu*[3], *Ken Sasaki*[4*]

[1]Hiroshima University, Higashi Hiroshima 739-8526, Japan
[2]University of Tsukuba, Tsukuba 305-8571, Japan
[3]Kyoto University, Kyoto 606-8501, Japan
[4]Yokohama National University, Yokohama 240-8501, Japan

DOI: http://dx.doi.org/10.3204/DESY-PROC-2009-03/Sasaki

We analyze the heavy quark mass effects on the virtual photon structure functions up to the NLO in the framework based on the operator product expansion supplemented by the mass-independent renormalization group method. We also investigate the target mass corrections for the virtual photon structure functions up to the NNLO.

1 Introduction

In e^+e^- collision experiments, the cross section for the two-photon processes $e^+e^- \to e^+e^- +$ hadrons, shown in Fig.1, dominates over other processes such as the annihilation process $e^+e^- \to \gamma^* \to$ hadrons at high energies. In particular, the two-photon processes in the double-tag events, where one of the virtual photon is very far off shell (large $Q^2 \equiv -q^2$) while the other is close to the mass shell (small $P^2 \equiv -p^2$), can be viewed as deep-inelastic electron-photon scattering and provide us the information on the structure of the photon.

In fact, the study of the photon structure has been an active field of research [1]. Recently we analyzed the photon structure function F_2^γ up to the next-to-next-to-leading order (NNLO) and F_L^γ up to the next-to-leading order (NLO) in perturbative QCD (pQCD) in the kinematical region $\Lambda^2 \ll P^2 \ll Q^2$, where Λ is the QCD scale parameter [2]. The interest of studying the photon structure in this kinematical region is that a definite prediction of the whole structure function, its shape and magnitude, may become possible. However, the above investigation of F_2^γ and F_L^γ has two flaws that need to be fixed. One is that we have treated all the quarks as massless. The other is that we have considered the logarithmic corrections arising from QCD higher-order effects, but ignored all the power corrections of the form $(P^2/Q^2)^k \quad (k = 1, 2, \cdots)$ coming from target mass effects.

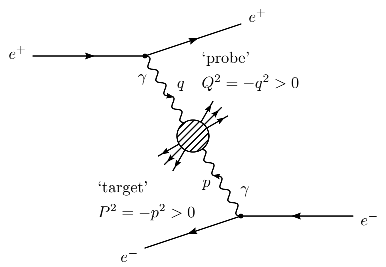

Figure 1: Deep-inelastic scattering on a virtual photon in the e^+e^- collider experiments

*Presented by Ken Sasaki

In this paper we discuss two topics which we have investigated recently, namely, heavy quark mass effects [4] and target mass effects [3] on the virtual photon structure functions. Heavy quark mass effects for the real photon were studied in the literature [5, 6].

2 Master formula for the moments with heavy quark

For the first topic, heavy quark mass effects, we consider the system which consists of $n_f - 1$ massless quarks and one heavy quark $q^{n_f} = q_H$ together with gluons and photons. The extension to the case with more heavy quarks is straightforward. Applying the operator product expansion (OPE) for the product of two electromagnetic currents at short distance we get

$$\begin{aligned} i\int d^4x e^{iqx} T(J_\mu(x)J_\nu(0)) &= \left(g_{\mu\nu} - \frac{q_\mu q_\nu}{q^2}\right) \sum_{\substack{n=0\\ n=\text{even}}} \left(\frac{2}{Q^2}\right)^n q_{\mu_1}\cdots q_{\mu_n} \sum_i C^i_{L,n} O_i^{\mu_1\cdots\mu_n} \\ &+ \left(-g_{\mu\lambda}g_{\nu\sigma}q^2 + g_{\mu\lambda}q_\nu q_\sigma + g_{\nu\sigma}q_\mu q_\lambda - g_{\mu\nu}q_\lambda q_\sigma\right) \\ &\times \sum_{\substack{n=2\\ n=\text{even}}} \left(\frac{2}{Q^2}\right)^n q_{\mu_1}\cdots q_{\mu_{n-2}} \sum_i C^i_{2,n} O_i^{\lambda\sigma\mu_1\cdots\mu_{n-2}} + \cdots , \end{aligned} \tag{1}$$

where $C^i_{L,n}$ and $C^i_{2,n}$ are the coefficient functions which contribute to the structure functions F_L^γ and F_2^γ, respectively, and $O_i^{\mu_1\cdots\mu_n}$ and $O_i^{\lambda\sigma\mu_1\cdots\mu_{n-2}}$ are spin-n twist-2 operators (hereafter we often refer to $O_i^{\mu_1\cdots\mu_n}$ as O_i^n). The sum on i runs over the possible twist-2 operators and $\cdots$ represents other terms with irrelevant coefficient functions and operators.

Let us denote $n_f - 1$ massless quarks as a column vector $\psi = (q^1, q^2, \cdots, q^{n_f-1})^{\mathrm{T}}$. Then the relevant operators in quark sector are light-flavour-singlet quark (L), heavy quark (H) and light-flavour-nonsinglet quark (NS) operators as follows:

$$O_L^{\mu_1\cdots\mu_n} = i^{n-1}\overline{\psi}\gamma^{\{\mu_1}D^{\mu_2}\cdots D^{\mu_n\}}\mathbf{1}\psi - \text{trace terms} , \tag{2a}$$
$$O_H^{\mu_1\cdots\mu_n} = i^{n-1}\overline{q}_H\gamma^{\{\mu_1}D^{\mu_2}\cdots D^{\mu_n\}}q_H - \text{trace terms} , \tag{2b}$$
$$O_{NS}^{\mu_1\cdots\mu_n} = i^{n-1}\overline{\psi}\gamma^{\{\mu_1}D^{\mu_2}\cdots D^{\mu_n\}}(Q^2_{ch} - \langle e^2\rangle_{(n_f-1)}\mathbf{1})\psi - \text{trace terms} , \tag{2c}$$

where $\{\ \ \}$ means complete symmetrization over the Lorentz indices $\mu_1\cdots\mu_n$ and D^μ denotes covariant derivative. In quark operators O_L^n and O_{NS}^n given in Eqs.(2a) and (2c), $\mathbf{1}$ is an $(n_f-1)\times(n_f-1)$ unit matrix, Q^2_{ch} is the square of the $(n_f-1)\times(n_f-1)$ quark-charge matrix, and $\langle e^2\rangle_{(n_f-1)} = (\sum_i^{n_f-1} e_i^2)/(n_f-1)$ is the average charge squared of massless quarks. Note that we have a relation $\mathrm{Tr}(Q^2_{ch} - \langle e^2\rangle_{(n_f-1)}\mathbf{1}) = 0$. Due to this relation, the operator O^n_{NS} does not mix with operators O^n_L and O^n_H. In addition to the above quark operators, the gluon (O^n_G) and photon (O^n_γ) operators are also relevant and appear in the r.h.s. of Eq.(1). Here the importance of inclusion of the heavy quark operator should be stressed. We treat the heavy quark in the same way as the light quarks and assume that both heavy and light quarks are radiatively generated from the photon target. In contrast, in the case of the nucleon target, heavy quarks are treated as radiatively generated from the gluon and light quarks.

The coefficient function $C^i_{k,n}(k = 2, L)$ corresponding to the operators $O^n_i(i = L, H, G, NS, \gamma)$ satisfies the following mass-independent renormalization group (RG) equation:

$$\left[\mu\frac{\partial}{\partial\mu} + \beta(g)\frac{\partial}{\partial g} + \gamma_m(g)m\frac{\partial}{\partial m} - \gamma_n(g,\alpha)\right]_{ij} C^j_{k,n}\left(\frac{Q^2}{\mu^2}, \frac{m^2}{\mu^2}, \bar{g}(\mu^2), \alpha\right) = 0 , \tag{3}$$

with $i, j = L, H, G, NS, \gamma$. Here $\beta(g)$ and $\gamma_m(g)$ are the beta function and the anomalous dimension for the mass operator, respectively, and $\gamma_n(g, \alpha)$ is a 5×5 anomalous dimension matrix. To the lowest order in the QED coupling constant α, this matrix has the following form:

$$\gamma_n(g,\alpha) \equiv \begin{pmatrix} \hat{\gamma}_n(g) & 0 \\ \boldsymbol{K}_n(g,\alpha) & 0 \end{pmatrix}, \quad \hat{\gamma}_n \equiv \begin{pmatrix} \gamma^n_{LL} & \gamma^n_{HL} & \gamma^n_{GL} & 0 \\ \gamma^n_{LH} & \gamma^n_{HH} & \gamma^n_{GH} & 0 \\ \gamma^n_{LG} & \gamma^n_{HG} & \gamma^n_{GG} & 0 \\ 0 & 0 & 0 & \gamma^n_{NS} \end{pmatrix}, \tag{4}$$

and $\boldsymbol{K}_n(g, \alpha)$ is the four-component row vector

$$\boldsymbol{K}_n = (K^n_L, K^n_H, K^n_G, K^n_{NS}) , \tag{5}$$

which describes the mixing between the photon operator and the remaining hadronic operators. The solution to the RG equation (3) is given by

$$C^i_{k,n}\left(\frac{Q^2}{\mu^2}, \frac{m^2}{\mu^2}, \bar{g}(\mu^2), \alpha\right) = \left\{ T \exp\left[\int_{\bar{g}(Q^2)}^{\bar{g}(\mu^2)} dg \frac{\gamma_n(g,\alpha)}{\beta(g)}\right]\right\}_{ij} C^j_{k,n}\left(1, \frac{\bar{m}^2(Q^2)}{Q^2}, \bar{g}(Q^2), \alpha\right) , \tag{6}$$

with $\bar{g}(\mu^2)$ being effective running QCD coupling constant and $\bar{m}(Q^2)$ is the running heavy quark mass evaluated at Q^2.

The matrix elements of the relevant operators O^n_i sandwiched by the photon states with momentum p are expressed as

$$\begin{aligned} \langle\gamma(p)|O^{\mu_1\cdots\mu_n}_i|\gamma(p)\rangle &= A^i_n\Big(\frac{P^2}{\mu^2}, \frac{\bar{m}^2(\mu^2)}{\mu^2}, \bar{g}(\mu^2)\Big)\ \{p^{\mu_1}\cdots p^{\mu_n}\ -\ \text{trace terms}\} \\ &\equiv A^i_n\Big(\frac{P^2}{\mu^2}, \frac{\bar{m}^2(\mu^2)}{\mu^2}, \bar{g}(\mu^2)\Big)\ \{p^{\mu_1}\cdots p^{\mu_n}\}_n , \end{aligned} \tag{7}$$

with $i = L, H, G, NS, \gamma$, and A^i_n is the reduced photon matrix element with μ being the renormalization point. Then the moment sum rules for the virtual photon structure functions F^γ_2 and F^γ_L are given by $(k = 2, L)$

$$\begin{aligned} M^\gamma_k(n, Q^2, P^2) &= \int_0^1 dx x^{n-2} F^\gamma_k(x, Q^2, P^2) \\ &= \sum_{i=L,H,G,NS,\gamma} A^i_n\Big(\frac{P^2}{\mu^2}, \frac{\bar{m}^2(\mu^2)}{\mu^2}, \bar{g}(\mu^2)\Big) C^i_{k,n}\left(\frac{Q^2}{\mu^2}, \frac{m^2}{\mu^2}, \bar{g}(\mu^2), \alpha\right). \end{aligned} \tag{8}$$

Now using Eq.(6) and choosing $\mu^2 = P^2$, we obtain the master formula for the moments for the case when a heavy quark exists,

$$\begin{aligned} M^\gamma_k(n, Q^2, P^2) &= \sum_{i,j=L,H,G,NS,\gamma} A^i_n\left(1, \frac{\bar{m}^2(P^2)}{P^2}, \bar{g}(P^2)\right)\left\{T\exp\left[\int_{\bar{g}(Q^2)}^{\bar{g}(P^2)} dg \frac{\gamma_n(g,\alpha)}{\beta(g)}\right]\right\}_{ij} \\ &\qquad \times C^j_{k,n}\left(1, \frac{\bar{m}^2(Q^2)}{Q^2}, \bar{g}(Q^2), \alpha\right) . \end{aligned} \tag{9}$$

The heavy quark mass effects appear in the reduced photon matrix element A^i_n and the coefficient function $C^j_{k,n}$ as the running quark mass $\bar{m}$.

3 Heavy quark mass effects in QCD

We focus on the moments $M_2^\gamma(n,Q^2,P^2)$ and consider the heavy quark mass effects up to the NLO. We take the difference between $M_2^\gamma(n,Q^2,P^2)$ and the one for the case when all n_f quarks are massless,

$$\Delta M_2^\gamma(n,Q^2,P^2,\bar{m}^2) = M_2^\gamma(n,Q^2,P^2) - M_2^\gamma(n,Q^2,P^2)\Big|_{\text{massless}} . \tag{10}$$

We already know $M_2^\gamma(n,Q^2,P^2)\Big|_{\text{massless}}$ (actually, up to the NNLO). The 1-loop (4×4) anomalous dimension matrix $\hat{\gamma}_n^{(0)}$ in hadronic sector in Eq.(4) has four eigenvalues λ_L^n, $\lambda_\pm^n$ and λ_{NS}^n and we find $\lambda_L^n = \lambda_{NS}^n (= \gamma_{\psi\psi}^{(0),n} = \gamma_{NS}^{(0),n})$. Diagonalizing the matrix $\hat{\gamma}_n^{(0)}$, we evaluate $M_2^\gamma(n,Q^2,P^2)$ in Eq.(9) up to the NLO and obtain

$$\begin{aligned}\Delta M_2^\gamma(n,Q^2,P^2,\bar{m}^2) \;=\; & \frac{\alpha}{4\pi}\frac{1}{2\beta_0}\Bigg[\sum_{i=\pm,NS}\Delta\mathcal{A}_i^n\left[1-\left(\frac{\alpha_s(Q^2)}{\alpha_s(P^2)}\right)^{d_i^n}\right] \\ & +\sum_{i=\pm,NS}\Delta\mathcal{B}_i^n\left[1-\left(\frac{\alpha_s(Q^2)}{\alpha_s(P^2)}\right)^{d_i^n+1}\right]+\Delta\mathcal{C}^n\Bigg]+\mathcal{O}(\alpha_s) \;,\end{aligned} \tag{11}$$

where $d_i^n = \lambda_i^n/2\beta_0$ $(i=\pm,NS)$ with $\beta_0 = 11-(2/3)n_f$. In the massive quark limit, $\Lambda^2 \ll P^2 \ll m^2 \ll Q^2$, the explicit expressions of $\Delta\mathcal{A}_i^n, \Delta\mathcal{B}_i^n, \Delta\mathcal{C}^n$ are

$$\Delta\mathcal{A}_{NS}^n = -12\beta_0 e_H^2(e_H^2-\langle e^2\rangle_{n_f})(\Delta\tilde{A}_{nG}^\psi/n_f), \tag{12a}$$

$$\Delta\mathcal{A}_\pm^n = -12\beta_0 e_H^2\langle e^2\rangle_{n_f}(\Delta\tilde{A}_{nG}^\psi/n_f)\frac{\gamma_{\psi\psi}^{(0),n}-\lambda_\mp^n}{\lambda_\pm^n-\lambda_\mp^n}, \tag{12b}$$

$$\Delta\mathcal{B}_{NS}^n = 0, \qquad \Delta\mathcal{B}_\pm^n = 0, \qquad \Delta\mathcal{C}^n = 12\beta_0 e_H^4(\Delta\tilde{A}_{nG}^\psi/n_f) \;, \tag{12c}$$

where e_H is the heavy quark charge, $\langle e^2\rangle_{n_f} = \sum_{i=1}^{n_f} e_i^2/n_f$ is the average squared charge and

$$\begin{aligned}\Delta\tilde{A}_{nG}^\psi/n_f \;=\; & 2\Bigg[-\frac{n^2+n+2}{n(n+1)(n+2)}\ln\frac{\bar{m}^2}{P^2}+\frac{1}{n}-\frac{1}{n^2} \\ & +\frac{4}{(n+1)^2}-\frac{4}{(n+2)^2}-\frac{n^2+n+2}{n(n+1)(n+2)}\sum_{j=1}^{n}\frac{1}{j}\Bigg] .\end{aligned} \tag{13}$$

We see from Eq. (11) that in our approach, using the OPE and the RG equation, the heavy quark mass effects start to appear at the NLO, but not at the LO. Also for the longitudinal structure function $F_L^\gamma(x,Q^2,P^2)$, heavy quark mass effects do not appear in the LO ($\mathcal{O}(\alpha)$).

4 Numerical analysis

The structure functions of the virtual photon are derived from the double-tag measurements of the reaction $e^+e^- \to e^+e^- +$ hadrons. So far there exist only two experimental results

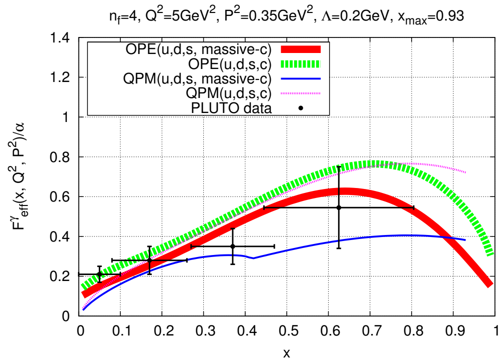

Figure 2: QCD and QPM predictions for $F_{\rm eff}^{\gamma}$ vs. PLUTO data

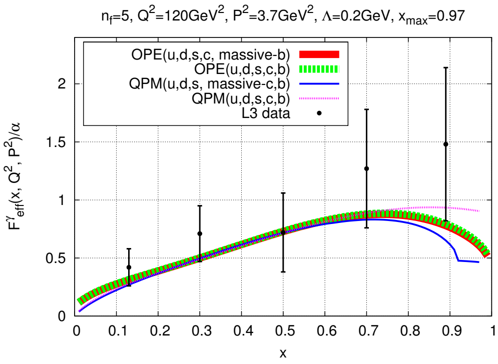

Figure 3: QCD and QPM predictions for $F_{\rm eff}^{\gamma}$ vs. L3 data

reported: one from the PLUTO Collaboration [7] and the other from the L3 Collaboration [8]. Both collaborations measured an effective photon structure function

$$F_{\rm eff}^{\gamma}(x,Q^2,P^2) = F_2^{\gamma}(x,Q^2,P^2) + \frac{3}{2}F_L^{\gamma}(x,Q^2,P^2)\ . \tag{14}$$

We evaluate $F_{\rm eff}^{\gamma}$ up to the NLO and compare our theoretical predictions with these data. The PLUTO (L3) data are at $Q^2 = 5\ (120)\ {\rm GeV}^2$ and $P^2 = 0.35\ (3.7)\ {\rm GeV}^2$. Therefore, we assume that the active flavours are u, d, s (massless) plus c (heavy) for the case of PLUTO and u, d, s, c (massless) plus b (heavy) for L3. We take the following values of the quark masses as inputs:

$$m_c = 1.3\ {\rm GeV} \quad (\text{for PLUTO}), \qquad m_b = 4.2\ {\rm GeV} \quad (\text{for L3}). \tag{15}$$

We plot $F_{\rm eff}^{\gamma}(x,Q^2,P^2)$ for $Q^2 = 5\ {\rm GeV}^2$ and $P^2 = 0.35\ {\rm GeV}^2$ together with the PLUTO data in Fig. 2. The thick red solid (green dashed) line represents the NLO QCD result with (without) charm quark mass effects. We have put $\Lambda = 0.2$ GeV. Although the condition $Q^2 \gg m_c^2$ is not satisfied, the predicted curve with mass effects shows a trend of reducing the "over-estimated" massless QCD calculation.

Also shown in Fig. 2 are the results by Quark Parton Model (QPM). In QPM $F_{\rm eff}^{\gamma}(x,Q^2,P^2)$ is expressed by the following four structure functions as

$$F_{\rm eff}^{\gamma}(x,Q^2,P^2) = \left(\frac{5}{\widetilde{\beta}^2} - 3\right)x\left[W_{TT} - \frac{1}{2}W_{TS}\right] + \frac{5}{\widetilde{\beta}^2}x\left[W_{ST} - \frac{1}{2}W_{SS}\right]\ , \tag{16}$$

where W_{TT}, W_{ST}, W_{TS}, and W_{SS} [9, 10] are functions of x and

$$\widetilde{\beta} = \sqrt{1 - \frac{P^2Q^2}{(p\cdot q)^2}}\ , \qquad \beta = \sqrt{1 - \frac{4m^2}{(p+q)^2}}\ , \qquad L = \ln\frac{1+\beta\widetilde{\beta}}{1-\beta\widetilde{\beta}}\ , \tag{17}$$

and charge factors $\delta_{\gamma}^{i} (= 3 \times e_i^4)$. The quark mass dependence resides in the parameter β. For the massless case we have $\beta = 1$. The thin blue solid (purple dashed) line represents the QPM result with (without) charm quark mass effects.

Figure 3 shows the results of $F_{\rm eff}^{\gamma}(x,Q^2,P^2)$ for $Q^2=120$ GeV^2 and $P^2=3.7$ GeV^2 together with the L3 data. In this case the condition $\Lambda^2 \ll P^2 \ll m_b^2 \ll Q^2$ is satisfied. The thick red solid line represents the NLO QCD prediction with bottom quark mass effects while the thick green dashed line shows the massless QCD result. Due to its charge factor, we see that the bottom quark mass effects are almost negligible. Also shown are the QPM results: the case for massive c and b (the thin blue solid line) and the case for massless u,d,s,c and b (the thin purple dashed line).

The heavy quark mass has an effect of reducing the photon structure functions in magnitude. This feature is explained by the suppression of the heavy quark production rate due to the existence of its mass. The kinematical constraint for the heavy quark production $(p+q)^2 \geq 4m^2$ gives $x_{\rm max}=\frac{1}{1+\frac{4m^2}{Q^2}+\frac{P^2}{Q^2}}$ below which the contribution of heavy quark to the structure functions exists and, therefore, the difference between the cases of massive and massless quark emerges above $x_{\rm max}$. This kinematical "threshold" effect is not clearly seen in our analysis since we adopted the framework based on the OPE and took into account only the leading twist-2 operators. But still we see in Fig. 2 that the difference between the two becomes bigger at larger x. It is also noted that the heavy quark mass effects are sensitive to the electric charge of the relevant quark. The photon structure functions depend on the quark-charge factors $\langle e^2\rangle$ and $\langle e^4\rangle$. Thus, as we see from Figs. 2 and 3, the up-type heavy quark has larger effects than the down-type heavy quark.

5 Target mass effects

For the case of massless quarks, we have studied in Ref.[2] the virtual photon structure functions $F_2^{\gamma}(x,Q^2,P^2)$ and $F_L^{\gamma}(x,Q^2,P^2)$ in pQCD for the kinematical region $\Lambda^2 \ll P^2 \ll Q^2$. There we have considered the logarithmic corrections arising from QCD higher-order effects, but ignored all the power corrections of the form $(P^2/Q^2)^k \quad (k=1,2,\cdots)$ coming either from target mass effects or from higher-twist effects. In fact, if the target is real photon ($P^2=0$), there is no need to consider target mass corrections. But when the target becomes off-shell ($P^2 \neq 0$) and for relatively low values of Q^2, contributions suppressed by powers of P^2/Q^2 may become important. Then we need to take into account these target mass contributions. The consideration of target mass effects (TME) is important by another reason. In the case of massless quarks, the maximal value of the Bjorken variable x for the virtual photon target is not 1 but $x_{\rm max}=\frac{1}{1+\frac{P^2}{Q^2}}$, due to the constraint $(p+q)^2 \geq 0$, which is in contrast to the nucleon case where $x_{\rm max}=1$. The structure functions should vanish at $x=x_{\rm max}$. However, the NNLO QCD results [2] for $F_2^{\gamma}(x,Q^2,P^2)$ as well as $F_L^{\gamma}(x,Q^2,P^2)$ show that the predicted graphs do not vanish but remains finite at $x=x_{\rm max}$. This flaw is coming from the fact that TME have not been taken into account in the analysis.

As the second topic, we show TME for the virtual photon structure functions $F_2^{\gamma}(x,Q^2,P^2)$ up to the NNLO and $F_L^{\gamma}(x,Q^2,P^2)$ up to the NLO in QCD in the framework of the OPE. The photon matrix elements of the relevant traceless operators in the OPE are expressed by traceless tensors. These tensors contain many trace terms so that they satisfy the tracelessness conditions. The basic idea for computing the target mass corrections is to take account of these trace terms in the traceless tensors properly.

The operators which appear in the OPE in Eq.(1) are traceless and have totally symmetric Lorentz indices $\mu_1\cdots\mu_n$ $(\lambda\sigma\mu_1\cdots\mu_{n-2})$. Hence $\{p^{\mu_1}\cdots p^{\mu_n}\}_n$, which emerges in the photon matrix elements of these operators in Eq.(7), is the totally symmetric rank-n tensor formed with the momentum p alone and satisfies the traceless condition $g_{\mu_i\mu_j}\{p^{\mu_1}\cdots p^{\mu_n}\}_n=0$. When we take the spin-averaged photon matrix element of the both sides of Eq.(1), we need to evaluate the contraction between $q_{\mu_1}\cdots q_{\mu_n}$ and the traceless tensors without neglecting any of the trace terms. The results are expressed in terms of Gegenbauer polynomials [11]:

$$q_{\mu_1}\cdots q_{\mu_n}\{p^{\mu_1}\cdots p^{\mu_n}\}_n = a^n C_n^{(1)}(\eta) \ , \tag{18a}$$

$$q_{\mu_1}\cdots q_{\mu_{n-2}}\{p^\lambda p^\sigma p^{\mu_1}\cdots p^{\mu_{n-2}}\}_n = \frac{1}{n(n-1)}\left[\frac{g^{\lambda\sigma}}{Q^2}a^n 2C_{n-2}^{(2)}(\eta) + \frac{q^\lambda q^\sigma}{Q^4}a^n 8C_{n-4}^{(3)}(\eta) + p^\lambda p^\sigma a^{n-2}2C_{n-2}^{(3)}(\eta) + \frac{p^\lambda q^\sigma + q^\lambda p^\sigma}{Q^2}a^{n-1}4C_{n-3}^{(3)}(\eta)\right], \tag{18b}$$

where

$$a = -\frac{1}{2}PQ, \quad \eta = -\frac{p\cdot q}{PQ} \ , \tag{19}$$

and $C_n^{(\nu)}(\eta)$'s are Gegenbauer polynomials. Then we obtain the Nachtmann moments [11], the weighted integrals of the structure functions F_2^γ and F_L^γ for the definite spin-n contributions, in stead of the familiar moments of F_2^γ and F_L^γ (see Eq.(8)),

$$M_2^\gamma(n,Q^2,P^2) = \int_0^{x_{\max}} dx\frac{1}{x^3}\xi^{n+1}\left[\frac{3+3(n+1)r+n(n+2)r^2}{(n+2)(n+3)}\right]F_2^\gamma(x,Q^2,P^2), \tag{20}$$

$$M_L^\gamma(n,Q^2,P^2) = \int_0^{x_{\max}} dx\frac{1}{x^3}\xi^{n+1}\left[F_L^\gamma(x,Q^2,P^2) + \frac{4P^2x^2}{Q^2}\frac{(n+3)-(n+1)\xi^2P^2/Q^2}{(n+2)(n+3)}F_2^\gamma(x,Q^2,P^2)\right] \ , \tag{21}$$

where r and ξ are defined as

$$r \equiv \sqrt{1-\frac{4P^2x^2}{Q^2}} \ , \qquad \xi \equiv \frac{2x}{1+\sqrt{1-\frac{4P^2x^2}{Q^2}}} = \frac{2x}{1+r}. \tag{22}$$

The left hand sides of Eqs.(20) and (21) are expressed as

$$M_2^\gamma(n,Q^2,P^2) = \sum_i A_n^i(P^2,g)\ C_{2,n}^i(Q^2,P^2,g), \tag{23}$$

$$M_L^\gamma(n,Q^2,P^2) = \sum_i A_n^i(P^2,g)\ C_{L,n}^i(Q^2,P^2,g) \ , \tag{24}$$

respectively, and are calculable by pQCD. Since the maximal value of x is not 1 but $\frac{1}{1+\frac{P^2}{Q^2}}$, the allowed ranges of r and ξ turn out to be $r_{\min}\le r\le 1$ and $0\le\xi\le 1$, respectively, where $r_{\min}=r(x_{\max})=(1-P^2/Q^2)/(1+P^2/Q^2)$ and $\xi(x_{\max})=1$.

The inversion of the Nachtmann moments can be made to express the structure functions

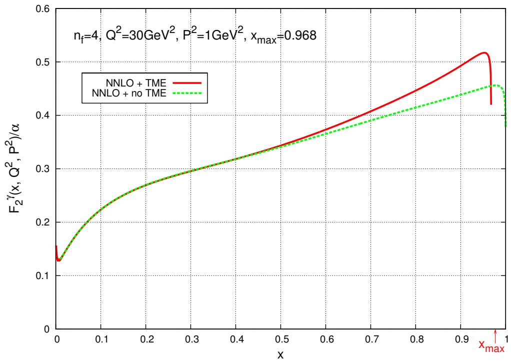

Figure 4: $F_2^\gamma(x, Q^2, P^2)$ with TME.

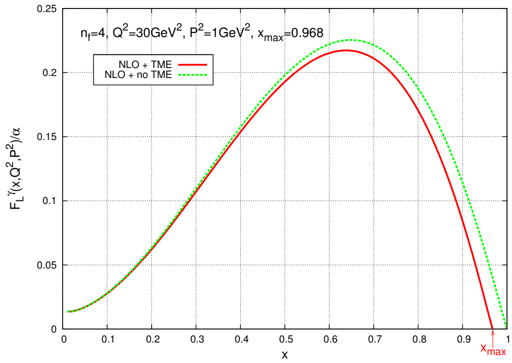

Figure 5: $F_L^\gamma(x, Q^2, P^2)$ with TME.

F_2^γ and F_L^γ explicitly as functions of x, Q^2 and P^2. Introducing the following functions,

$$G(\xi) \equiv \frac{1}{2\pi i}\int_{c-i\infty}^{c+i\infty} dn\, \xi^{-n+1}\frac{M_2^\gamma(n,Q^2,P^2)}{n(n-1)} \; , \tag{25a}$$

$$H(\xi) \equiv -\frac{dG(\xi)}{d\xi} = \frac{1}{2\pi i}\int_{c-i\infty}^{c+i\infty} dn\, \xi^{-n}\frac{M_2^\gamma(n,Q^2,P^2)}{n} \; , \tag{25b}$$

$$F(\xi) \equiv -\frac{dH(\xi)}{d\xi} = \frac{1}{2\pi i}\int_{c-i\infty}^{c+i\infty} dn\, \xi^{-n-1} M_2^\gamma(n,Q^2,P^2) \; , \tag{25c}$$

$$F_L(\xi) \equiv \frac{1}{2\pi i}\int_{c-i\infty}^{c+i\infty} dn\, \xi^{-n-1} M_L^\gamma(n,Q^2,P^2) \; , \tag{25d}$$

we find

$$F_2^\gamma(x,Q^2,P^2) = \frac{x^2}{r^3}F(\xi) - 6\kappa\frac{x^3}{r^4}H(\xi) + 12\kappa^2\frac{x^4}{r^5}G(\xi) \; , \tag{26}$$

$$F_L^\gamma(x,Q^2,P^2) = \frac{x^2}{r}F_L(\xi) - 4\kappa\frac{x^3}{r^2}H(\xi) + 8\kappa^2\frac{x^4}{r^3}G(\xi) \; . \tag{27}$$

Equations (26) and (27) are the final formulas for the photon structure functions F_2^γ and F_L^γ when target mass effects are taken into account.

We plot the graphs of $F_2^\gamma(x,Q^2,P^2)$ and $F_L^\gamma(x,Q^2,P^2)$ as functions of x in Fig.4 and Fig.5, respectively, for the case of $Q^2 = 30\text{GeV}^2$ and $P^2 = 1\text{GeV}^2$ with $x_{\max} = 0.968$. We take $\Lambda = 0.2$ GeV and $n_f = 4$ for the number of active quark flavours. The Bjorken variable x ranges from 0 to $x_{\max}$. We observe that TME become sizable at larger x region. While TME enhances F_2^γ at larger x, it reduces F_L^γ. The target mass correction is of order 10 % when compared at the maximal values for F_2^γ. In the case of F_L^γ, the maximal value is attained in the middle x, where the TME reduces the F_L^γ about 5 %.

6 Summary

Using the framework based on the OPE supplemented by the RG method, we investigated the heavy quark mass effects and also the target mass effects on the virtual photon structure functions. As for the heavy quark effects, we assumed that heavy quark is generated radiatively from the target photon as well as light quarks. In terms of the OPE terminology, we included the heavy quark operator. Then, the heavy quark mass effects appear in the reduced photon matrix element of this operator and also in the coefficient functions. We evaluated $F_{\rm eff}^{\gamma}(x, Q^2, P^2)$ with quark mass effects up to the NLO and compared our results with the PLUTO and L3 data.. The predicted curve with charm quark mass effects in Fig. 2 shows a right trend of reducing the "over-estimated" massless QCD calculation. As we see in Fig. 3, the bottom quark mass effects are almost negligible due to its charge factor.

When we study the virtual photon structure functions in the framework based on the OPE we also need to consider target mass corrections. We derived the Nachtmann moments for the structure functions and then, by inverting the moments, we obtained the expressions in closed form for $F_2^{\gamma}(x, Q^2, P^2)$ and $F_L^{\gamma}(x, Q^2, P^2)$, both of which include the target mass corrections. We observe that the target mass effects appear at larger x and become sizable near $x_{\rm max}$.

References

[1] M. Krawczyk, A. Zembrzuski and M. Staszel, Phys. Rep. **345** 265 (2001); R. Nisius, Phys. Rep. **332** 165 (2001); M. Klasen, Rev. Mod. Phys. **74** 1221 (2002).

[2] T. Ueda, K. Sasaki and T. Uematsu, Phys. Rev. **D75** 114009 (2007).

[3] Y. Kitadono, K. Sasaki, T. Ueda and T. Uematsu, Prog. Theor. Phys. **121** 495 (2009).

[4] Y. Kitadono, K. Sasaki, T. Ueda and T. Uematsu, Phys. Rev. **D77** 054019 (2008).

[5] M. Glück and E. Reya, Phys. Rev. **D28** 2749 (1983); M. Glück, E. Reya and A. Vogt, Phys. Rev. **D46** 1973 (1992); M. Glück, E. Reya and C. Sieg, Phys. Lett. **B503** 285 (2001); Eur. Phys J. C **20** 271 (2001); M .Glück, E. Reya and I. Schienbein, Phys. Rev. **D60** 054019 (1999); Phys. Rev. **D63** 074008 (2001); I. Schienbein, Annals of Physics, **301** 128 (2002).

[6] F. Cornet, P. Jankowski, M. Krawczyk and A. Lorca, Phys. Rev. **D68** 014010 (2003); F. Cornet, P. Jankowski and M. Krawczyk, Phys. Rev. **D70** 093004 (2004).

[7] Ch. Berger *et al.*, Phys. Lett. **B142** 119 (1984).

[8] M. Acciarri *et al.*, Phys. Lett. **B483** 373 (2000).

[9] V.M. Budnev, I.F. Ginzburg, G.V. Meledin and V.G. Serbo, Phys. Rep. **15** 181 (1974).

[10] K. Sasaki, J. Soffer and T. Uematsu, Phys. Rev. **D66** 034014 (2002).

[11] O. Nachtmann, Nucl. Phys. **B63** 237 (1973); **B78** 455 (1974).